

Disruption of Trp53 in Livers of Mice Induces Formation of Carcinomas With Bilineal Differentiation

SARAH-FEE KATZ,* ANDRÉ LECHER,* ANNA C. OBENAUFG,† YVONNE BEGUS-NAHRMANN,* JOHANN M. KRAUS,§ EVA M. HOFFMANN,‡ JOHANNA DUDA,|| PARISA ESHRAGHI,* DANIEL HARTMANN,*[¶] BIRGIT LISS,|| PETER SCHIRMACHER,[#] HANS A. KESTLER,[§] MICHAEL R. SPEICHER,[‡] and K. LENHARD RUDOLPH*

*Institute of Molecular Medicine and Max Planck Research Group on Stem Cell Aging, §Research Group Bioinformatics & Systems Biology, Institute of Neural Information Processing, and ||Research Group on Molecular Neurophysiology, University of Ulm, Ulm, Germany; ‡Institute of Human Genetics, Medical University of Graz, Graz, Austria; ¶Department of Surgery, Technical University Munich, Munich, Germany; and ¶Institute of Pathology, University of Heidelberg, Heidelberg, Germany

See editorial on page 1066.

BACKGROUND & AIMS: p53 limits the self-renewal of stem cells from various tissues. Loss of p53, in combination with other oncogenic events, results in aberrant self-renewal and transformation of progenitor cells. It is not known whether loss of p53 is sufficient to induce tumor formation in liver. **METHODS:** We used *AlfpCre* mice to create mice with liver-specific disruption of *Trp53* (*AlfpCre⁺Trp53^{Δ2-10/Δ2-10}* mice). We analyzed colony formation and genomic features and gene expression patterns in liver cells during hepatocarcinogenesis in mice with homozygous, heterozygous, and no disruption of *Trp53*. **RESULTS:** Liver-specific disruption of *Trp53* consistently induced formation of liver carcinomas that had bilineal differentiation. In nontransformed liver cells and cultured primary liver cells, loss of p53 (but not p21) resulted in chromosomal imbalances and increased clonogenic capacity of liver progenitor cells (LPCs) and hepatocytes. Primary cultures of hepatocytes and LPCs from *AlfpCre⁺Trp53^{Δ2-10/Δ2-10}* mice, but not *Cdkn1a^{-/-}* mice, formed tumors with bilineal differentiation when transplanted into immunocompromised mice. Spontaneous liver tumors that developed in *AlfpCre⁺Trp53^{Δ2-10/Δ2-10}* mice had significant but complex alterations in expression of Rb checkpoint genes compared with chemically induced liver tumors that developed mice with wild-type *Trp53*. **CONCLUSIONS: Deletion of p53 from livers of mice is sufficient to induce tumor formation. The tumors have bilineal differentiation and dysregulation of Rb checkpoint genes.**

Keywords: Liver Cancer; Cancer Stem Cell; Tumor Suppressor.

The p53 checkpoint function represents one of the most relevant tumor suppressor mechanisms in humans.¹ In addition to its role in p53 checkpoint control, p53 influences cellular differentiation and stem cell function. p53 induces differentiation of embryonic stem cells, whereas loss of p53 can increase the formation of pluripotent stem cells.^{2–6} In various somatic tissues, p53 re-

stricts self-renewal of adult stem cells, including hematopoietic, neuronal, and breast epithelial stem cells.^{7–9}

In human cancer, p53 mutations are associated with poorly differentiated tumors, including hepatocellular carcinoma (HCC).^{10,11} Vice versa, the reintroduction of p53 has been shown to induce differentiation of tumor cells.¹² Dedifferentiation of p53-mutant tumors could point to a stem cell origin of the tumors. In agreement with this hypothesis, it has been shown that p53 restricts the aberrant self-renewal of stem and progenitor cells carrying oncogenic alterations, specifically that p53 deletion promotes self-renewal of myeloid progenitor cells expressing oncogenic *Kras^{G12D}*.¹³ Similarly, p53 deficiency cooperates with *Pten* inactivation to promote aberrant self-renewal of neural progenitor cells.¹⁴ In these scenarios, increases in progenitor cell self-renewal resulted in higher frequencies of leukemia or glioblastoma formation. p53 deletion may also lead to transformation by inducing dedifferentiation and reprogramming of differentiated organ cells.¹⁵

In addition to the possible impact of p53 on dedifferentiation and stem cell self-renewal, it remains an open question whether loss of p53 alone is sufficient to induce cancer in solid organs. Mutations in the p53 gene occur in approximately 20% of HCCs, but more than 50% of aflatoxin-induced HCCs show p53 mutations as an early molecular event.^{16–19}

There is evidence that liver tumors with features of mixed differentiation occur in 20%–30% of patients^{20–22} and may show similarities to stem and progenitor cells in gene expression profiles.^{11,23,24} These findings have fueled the discussion whether stem and progenitor cells could represent the cell type of origin of liver cancer formation.

Here we analyzed consequences of hepatic deletion of p53 in adult mouse liver. The study provides the first experimental evidence that p53 deletion as a single genetic lesion can lead to formation of liver tumors with bilineal

Abbreviations used in this paper: aCGH, array-comparative genomic hybridization; DEN, diethylnitrosamine; LPC, liver progenitor cell.

© 2012 by the AGA Institute

0016-5085/\$36.00

doi:10.1053/j.gastro.2012.02.009

differentiation and altered Rb checkpoint gene expression.

Materials and Methods

Mouse Models

Conditional *Trp53^{F2-10/F2-10}* knockout mice²⁵ were crossed with *AlfpCre* transgenic mice.²⁶ The following experimental cohorts on the C57BL/6J background were generated: *AlfpCre⁺Trp53^{Δ2-10/Δ2-10}* = *p53^{-/-}*, *AlfpCre⁺Trp53^{Δ2-10/+}* = *p53^{+/-}*, and *AlfpCre⁻Trp53^{F2-10/F2-10}* = *p53^{+/+}*. Additionally, we used *Cdkn1a^{-/-}* mice (*p21^{-/-}*).²⁷ NMRI nu/nu mice or NOD-scid IL2Rg^{null} mice were used for transplantation assays. The animals were maintained in a specific pathogen-free environment and monitored weekly for tumor formation. Cells were subcutaneously injected with 25% Matrigel (BD Biosciences, San Jose, CA) into 4- to 6-week-old mice. All animal experiments were approved by the state government of Baden-Württemberg (protocol number 35/9185.81-3/940).

Isolation of Cells From Adult Mouse Liver

Cells were isolated from postnatal mouse livers by 2-step collagenase perfusion. Liver progenitor cells (LPCs) were isolated by fluorescence-activated cell sorting as described in Supplementary Materials and Methods.²⁸ Hepatocytes were purified by centrifugation in 50% Percoll (50g for 10 minutes).

In Vitro Colony-Forming Assay

LPCs were single cell sorted onto collagen type I-coated 96-well plates and cultured as described in Supplementary Materials and Methods.²⁸ Colony numbers were analyzed 3 weeks after initiating the cultures.

Genome-Wide Amplification

Genome-wide amplification of DNA was performed as described previously (see Supplementary Materials and Methods).^{29,30}

Array-Comparative Genomic Hybridization

Array-comparative genomic hybridization (aCGH) was performed using a genome-wide oligonucleotide microarray platform (mouse genome CGH 44K or 180K microarray kit; Agilent Technologies, Santa Clara, CA). As reference DNA, we used male DNA from the same mouse strain. Samples were labeled with the Agilent Genomic DNA Labeling Kit (Agilent Technologies) according to the manufacturer's instructions. Slides were scanned using a microarray scanner, and images were analyzed using DNA Analytics 4.0 (both from Agilent Technologies) with the statistical algorithm ADM-2.

Microarray Analysis

Gene expression analysis was performed using the Mouse GE 4x44Kv2 Microarray Kit (Agilent Technologies). Samples were labeled with the Quick Amp Labeling Kit (Agilent Technologies) according to the manufacturer's instructions. Slides were scanned using a microarray scanner (Agilent Technologies). All expression data were deposited in Gene Expression Omnibus (GEO accession number GSE34760).

Statistical Analysis

The χ^2 test, unpaired Student *t* test, and Fisher exact test were used for calculating statistical significance with GraphPad

Prism (GraphPad Software, Inc, La Jolla, CA) and R version 2.14 (<http://www.r-project.org>).

Further experimental procedures are given in Supplementary Materials and Methods.

Results

Homozygous Deletion of p53 as a Single Genetic Lesion Induces Liver Cancer Exhibiting Mixed Lineage Differentiation and Chromosomal Instability

To evaluate the role of p53 deletion in liver carcinogenesis, *Trp53^{F2-10/F2-10}* mice were crossed with transgenic mice expressing the Cre-recombinase under the liver-specific albumin/ α -fetoprotein enhancer promoter, which is activated on embryonic days 10–11.^{25,26} Homozygous deletion of p53 in mouse liver (*p53^{-/-}*) consistently led to tumor formation in 14- to 20-month-old mice (Figure 1A). Most of the mice developed liver cancer (Figure 1B). None of the *p53^{+/-}* mice and p21 knockout mice developed liver cancer (Figure 1A), indicating that formation of liver cancer in response to p53 deletion involves p21-independent mechanisms.

In agreement with previous studies on carcinogen-induced liver cancer,³¹ liver tumor formation was significantly accelerated in *p53^{-/-}* male compared with female mice (Supplementary Figure 1A). Macroscopically, liver tumors in *p53^{-/-}* mice were typically whitish and sclerotic (Figure 1C). Histologic analysis revealed ductular (bile ducts) and trabecular structures (hepatocytic) as well as a high stromal content (Figure 1D and E). Southern blot and quantitative reverse-transcription polymerase chain reaction analyses showed that these stromal cells were nontransformed, p53 wild-type cells (Supplementary Figure 1B–E). The *p53^{-/-}* livers did not exhibit premalignant lesions (eg, basophilic or clear cell foci) that are typically found in carcinogen-treated mouse liver.³² The earliest detectable, focal lesions in *p53^{-/-}* mouse livers were microscopically indistinguishable from advanced hepatocellular carcinoma/cholangiocellular carcinoma (HCC/CC) of older mice (Figure 1E). *p53^{-/-}* liver tumors expressed markers of cholangiocytic (K19-positive) and hepatocytic (albumin-positive) differentiation (Figure 1F) as well as the A6 epitope (Figure 1F), an uncharacterized epitope expressed by oval cells.^{33,34} Expression of α -fetoprotein was not detected (data not shown).

aCGH of DNA from whole tumor biopsy specimens revealed genomic imbalances. Loss of chromosomes 9 and 12 as well as gain of chromosome 15 were observed at a high frequency (Supplementary Figure 1F and Supplementary Table 1).

aCGH analysis of microscopic tumors indicated that these early tumors contain some chromosomal lesions (loss of chromosome 12, gain of chromosome 15) that are also present with high frequency in macroscopic tumors (Supplementary Table 1). These results support the histologic observation that microscopic tumors were similar to advanced tumors in *p53^{-/-}* liver. Nontransformed *p53^{-/-}* liver did not show evidence for clonal chromo-

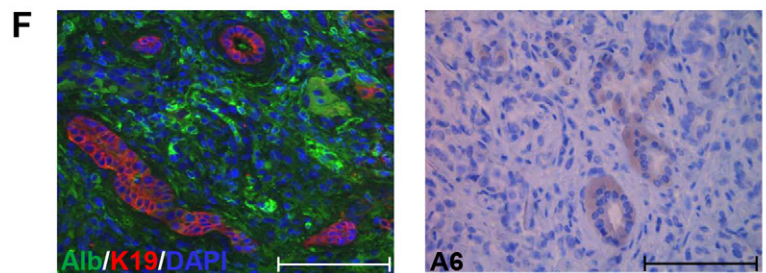
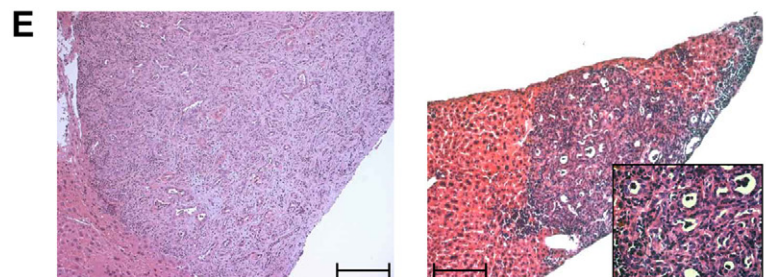
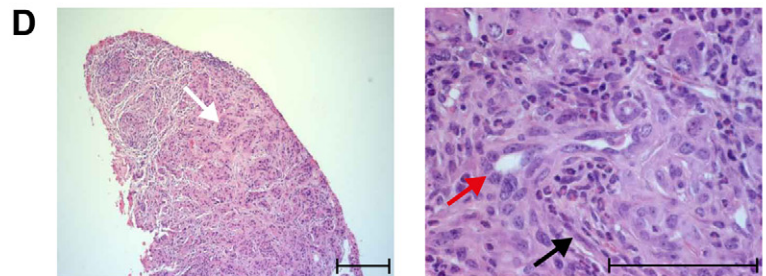
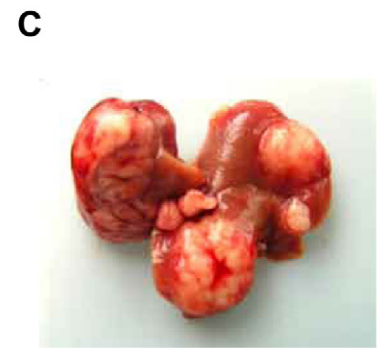
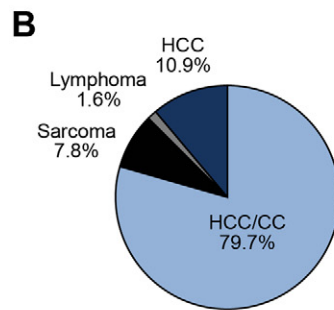
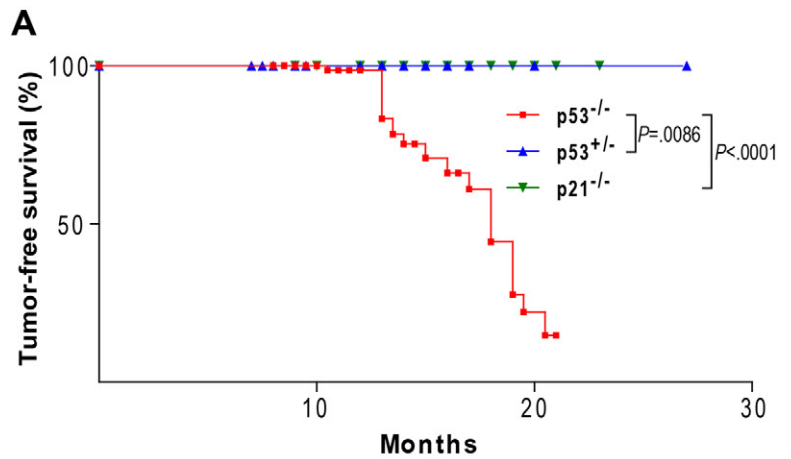


Figure 1. p53 deletion as a single genetic lesion leads to formation of liver carcinoma with bilineal differentiation features. (A) Tumor-free survival curve. Liver tumor formation was analyzed in mice with liver-specific homozygous (n = 94) and heterozygous p53 deletion (n = 47) and in germline p21 knockout mice (n = 22). (B) Spectrum of the histologically analyzed tumors. Liver carcinoma with hepatocytic and cholangiocytic differentiation (HCC/CC) (n = 51), liver carcinoma with only hepatocytic features (HCC) (n = 7), lymphoma (n = 1), and sarcoma (n = 5). (C) Macroscopic liver tumor in p53^{-/-} mice. (D) H&E-stained sections of mixed differentiated p53^{-/-} liver tumors showing hepatocytic differentiation (white arrow, left panel), ductular structure (red arrow, right panel), and stromal cells (black arrow, right panel). (E) H&E staining of an advanced liver tumor (left panel) and a macroscopically tumor-free liver carrying an early, microscopic liver tumor (right panel). (F) Representative immunofluorescence of the hepatocytic (albumin) and the cholangiocytic marker (K19) in p53^{-/-} liver tumors with bilineal differentiation (left panel). Representative immunohistochemistry of the oval cell marker A6 in p53^{-/-} liver tumors of bilineal differentiation (right panel). Scale bars = 100 μm.

somal aberrations (Supplementary Figure 1F). Chromosomal aberrations in chemically (diethylnitrosamine [DEN])-induced HCC in p53^{+/+} mice were distinct from those in spontaneous liver cancers in p53^{-/-} mice (Supplementary Table 1 and Supplementary Results).

Tumorigenicity of p53-Deficient Liver Carcinoma Does Not Depend on a Subpopulation of Tumor-Maintaining Cells

Recent studies revealed experimental evidence that the tumorigenicity of some tumors depends on a subpopulation of tumor cells.^{35,36} Quantitative real-time polymerase chain reaction and immunofluorescence staining revealed an increased expression of tumor stem cell markers in p53^{-/-} liver tumors compared with the surrounding, nontransformed liver (Supplementary Figure 2A-C). To functionally test the possible existence of a tumor-maintaining cellular subpopulation in p53^{-/-} liver carcinomas, freshly established cell cultures from liver tumors were purified using cancer stem cell surface markers as well as a functional marker (side population) (Table 1). Limiting dilution transplantation of cancer cell cultures into immunocompromised mice revealed a high tumor-forming capacity of p53^{-/-} liver carcinoma cells (1 of 15 cells formed tumors) independent of the tested marker (Table 1), indicating that these carcinomas did not depend on a subfraction of tumor-maintaining cells.

p53 Deletion Enhances Colony-Forming Capacity of Bipotent LPCs During Aging

The development of bilinear cancers in p53^{-/-} livers suggested that tumors may be derived from LPCs. Using recently established protocols,²⁸ progenitor cells were purified from livers of 2- to 3- and 8- to 10-month-old mice (Figure 2A) and sorted as single cells into 96-well plates. In agreement with previous publications,²⁸ a subset

of these purified single cells exhibited clonal expansion capacity (Figure 2B and C). Most of the colonies expressed only cholangiocytic marker (K19; Figure 2B), but some colonies showed a higher proliferation capacity and a mixed lineage differentiation into albumin and K19-expressing cells (Figure 2C). A small subset of cells exhibited coexpression of both markers.

Eight percent to 12% of the freshly purified LPCs had the capacity to form cholangiocytic colonies in cell culture (Figure 2D) with no significant effect of age or p53 genotype. A total of 0.55%–0.82% of the purified LPCs from 2- to 3-month-old mice exhibited bilinear differentiation capacity, which was not affected by p53 gene status (Figure 2E). p53-positive mice exhibited a strong age-dependent decline in LPCs to form bilinear colonies (only 0.045% of the sorted cells formed colonies with bilinear differentiation in 8- to 10-month-old mice; Figure 2E). In contrast, isolated LPCs from p53^{-/-} mice did not show a significant age-dependent decline in the capacity to form bilinear colonies (Figure 2E). Previous studies have shown that cells from these bilinear colonies can self-renew and exhibit bilinear colony-forming capacity at the single-cell level at later passage.²⁸

p21, a downstream target of p53, can affect stem cell self-renewal.^{37,38} Therefore, we analyzed LPCs from 8- to 10-month-old p21^{-/-} mice. Deletion of p21 was associated with a significant increase in colonies with bilinear differentiation (0.22% of sorted cells) compared with age-matched p53-positive mice (Figure 2E), but the number of bipotent progenitor cells remained reduced compared with age-matched p53^{-/-} mice. Together, these data indicated that p53 induces age-dependent restrictions in bilinear colony-forming capacity of LPCs involving p21-dependent and p21-independent mechanisms.

p53 Deletion Increases Clonogenic Capacity and Chromosomal Instability of LPCs and Differentiated Hepatocytes

p53 deletion also enhanced the capacity of bilinear and cholangiocytic colonies (derived from single sorted cells) to form cell lines (Supplementary Figure 3A). In vivo bromodeoxyuridine incorporation in LPCs did not reveal a significant difference in p53^{-/-} mice compared with p53-positive mice (Supplementary Figure 3B). However, the analysis could not exclude differences in the rate of proliferation in bipotent LPCs because the fraction of bipotent cells was less than 1% in this subpopulation of LPCs (see Figure 2).

To analyze the influence of p53 gene status on growth of differentiated liver cells, freshly isolated hepatocytes were cultivated. Hepatocytes isolated from 8-month-old p53^{-/-} mice were able to grow in vitro, whereas hepatocytes isolated from p53^{+/-}, p53^{+/+}, and p21^{-/-} mouse liver failed to proliferate and exhibited increased rates of cell death from day 14 after initiation of cultures, leading to complete loss of the cultures after 1–2 months (Supplementary Figure 4A and B). Primary hepatocyte cultures from p53^{-/-} liver showed a change in morphology over time, indicating that hepatocytes dedifferentiated and acquired mixed differentiation over time (Supplementary

Table 1. p53^{-/-} Liver Carcinoma Cells Exhibit a High Tumor-Forming Capacity Not Associated With a Specific Subpopulation of Tumor Cells

Marker	Cell number and tumor formation					
	5000	2000	500	50	10	2
CD133 ⁺	10/10	—	10/10	—	—	—
CD133 ⁻	10/10	—	10/10	—	—	—
CD90 ⁺	10/10	—	10/10	—	—	—
CD90 ⁻	4/4	—	10/10	—	—	—
CD13 ⁺	—	6/6	8/8	7/10	—	—
CD13 ⁻	—	6/6	8/8	10/10	—	—
cKit ⁺	—	—	8/8	9/10	—	—
cKit ⁻	—	—	10/10	10/10	—	—
SP	28/32	—	—	3/28	—	—
Non SP	27/28	—	—	19/28	—	—
Bulk	—	—	—	—	64/104	17/92

NOTE. Primary tumor cells were expanded from p53^{-/-} liver tumors and fluorescence-activated cell sorter purified using different surface markers (CD133, CD90, CD13, cKit) and a functional marker (side population). The table summarizes the tumor-forming capacity for the indicated number of transplanted cells from the indicated subpopulations of tumor cells.

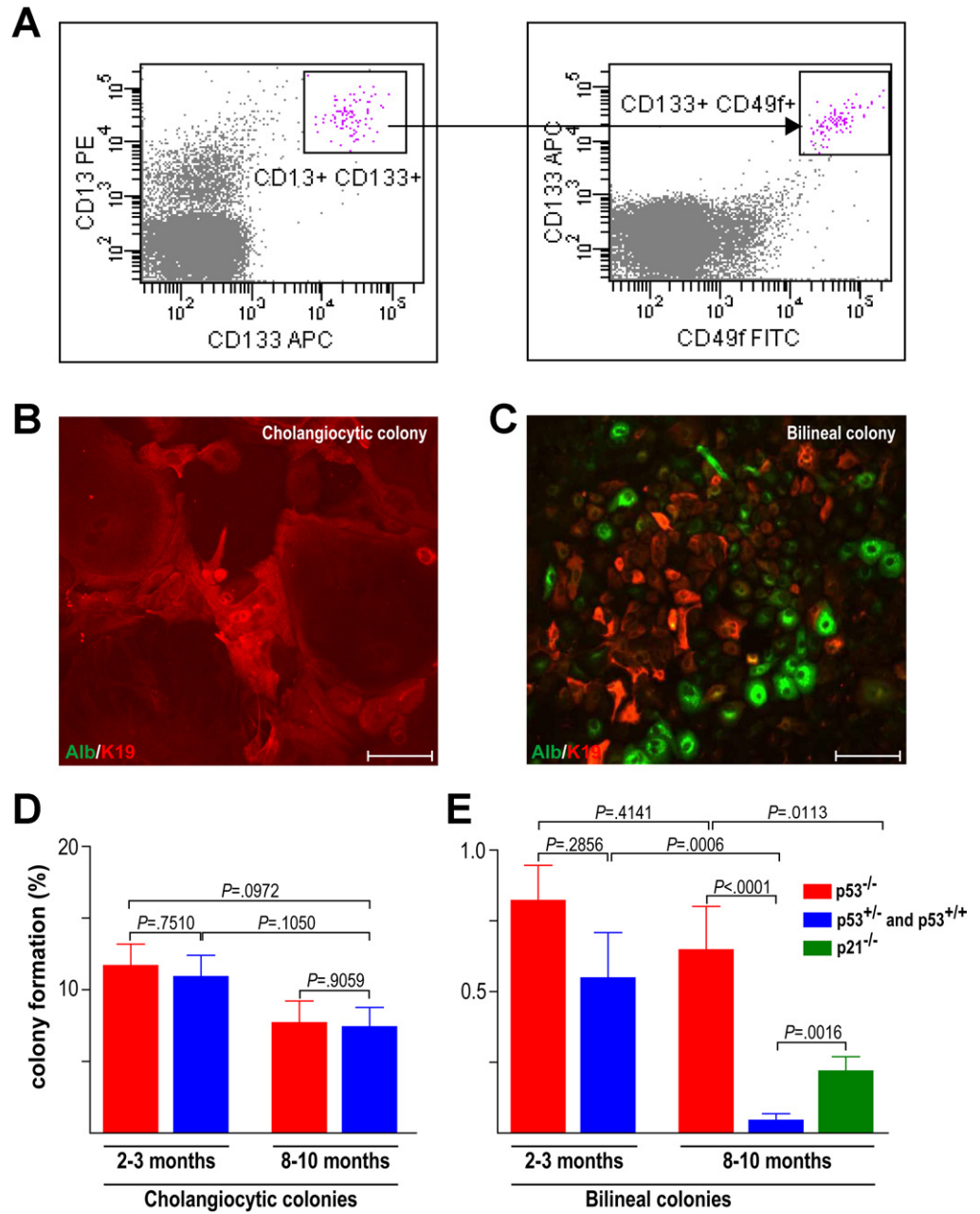


Figure 2. p53 deletion prolongs self-renewal of bipotent progenitor cells in adult mouse liver. (A) Representative fluorescence-activated cell sorting plot diagrams of nonparenchymal liver cells. Squares indicate the gates for sorting of LPCs (CD13⁺, CD133⁺, CD49f⁺). (B and C) Immunofluorescence of colonies derived from single LPCs for cholangiocytic (K19) and hepatocytic (albumin) markers demonstrating colonies with (B) cholangiocytic and (C) bilineal differentiation. Scale bars = 100 μm. (D and E) Bar graphs show the colony-forming capacity of LPCs depicting the percentage of cells that can form (D) cholangiocytic colonies or (E) bilineal differentiated colonies.

Figure 5). The observed changes occurred quickly and in a high percentage of cultured cells, indicating that p53^{-/-} hepatocytes changed differentiation stage. In contrast, p53^{+/+} hepatocytes did not survive a prolonged culture period and did not exhibit a strong coexpression of those 2 markers until day 14 of culture (Supplementary Figure 6). In vivo bromodeoxyuridine labeling indicated that loss of p53 impairs the induction/maintenance of hepatocyte quiescence in vivo (Figure 3A).

Maintenance of chromosomal stability represents another function of p53 contributing to tumor suppression.³⁹⁻⁴² There is emerging evidence that loss of p53 checkpoint function can lead to chromosomal instability in stem cells, especially in the context of other genomic insults, such as telomere dysfunction.^{5,41,43,44} Here, aCGH analysis revealed that a significantly increased number of freshly isolated progenitor

cells (10/28) from nontumorous livers of p53^{-/-} mice carried chromosomal imbalances compared with p53-positive and p21^{-/-} LPCs (2/36; Figure 3B and C, Supplementary Table 2, and Supplementary Results). Freshly isolated hepatocytes from p53^{-/-} liver represented genomic imbalances similar to p53^{-/-} progenitor cells (3/25; Figure 3B and C, Supplementary Table 2, and Supplementary Results). An increased rate of chromosomal aberrations was also present in primary colonies derived from single cell-sorted, freshly isolated p53^{-/-} LPCs (10/20; Figure 3B and C) compared with colonies from p53-positive (1/16; Figure 3C) and p21^{-/-} mice (1/12; Figure 3B and C, Supplementary Table 2, and Supplementary Results). Together, these data showed that loss of p53 function is associated with

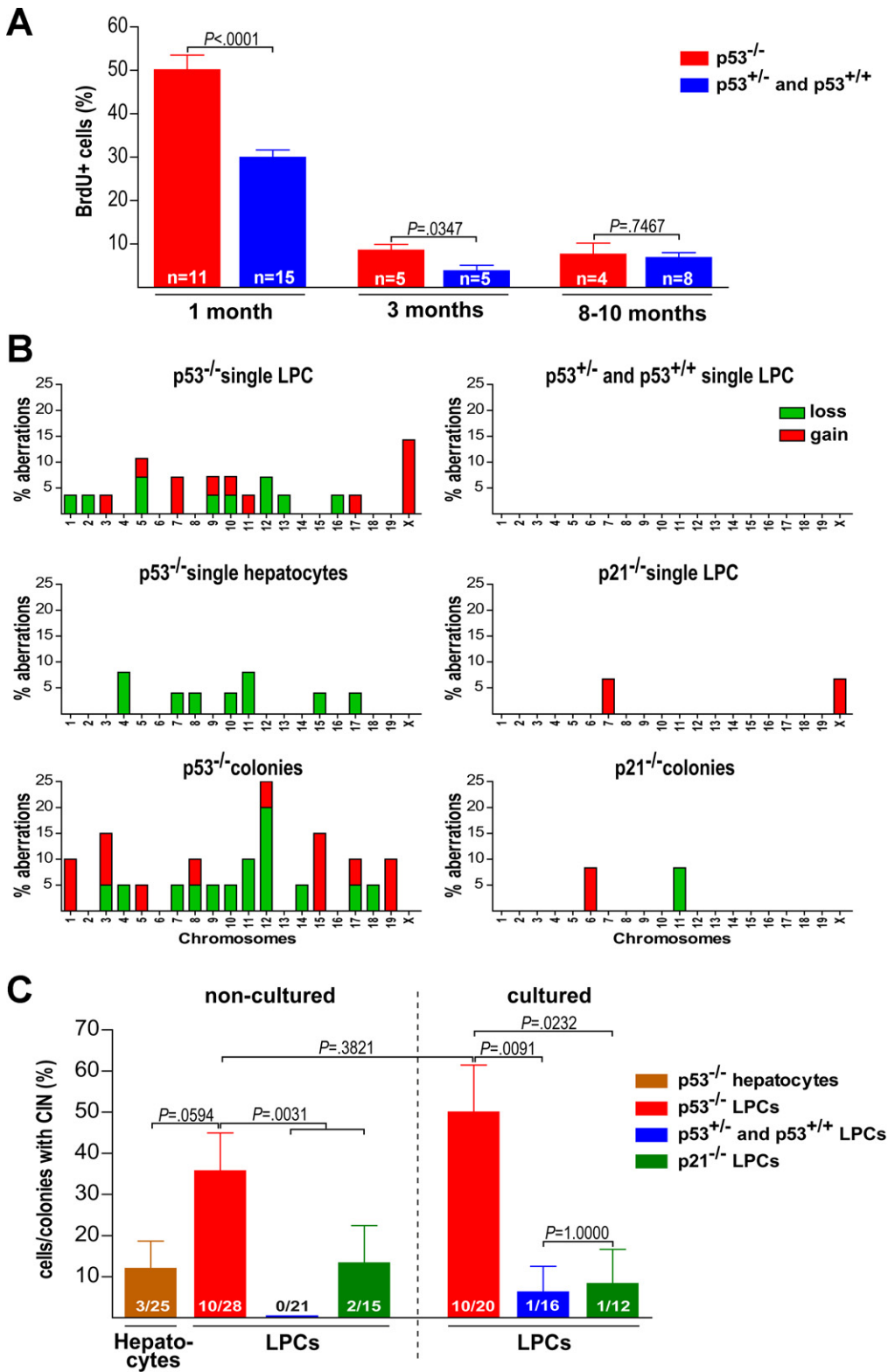


Figure 3. p53 deletion induces proliferation of hepatocytes and induces genomic instability of LPCs and differentiated hepatocytes. (A) Bromodeoxyuridine-positive hepatocytes after continuous bromodeoxyuridine labeling. (B) Chromosomal aberrations were analyzed by aCGH in single, freshly isolated LPCs, differentiated hepatocytes, and primary colonies derived from single LPCs from 8- to 10-month-old mice. The bar graphs of the denoted genotypes summarize genomic imbalances. (C) Percentage of single freshly isolated cells (noncultured) and colonies derived from single LPCs (cultured) with chromosomal imbalances.

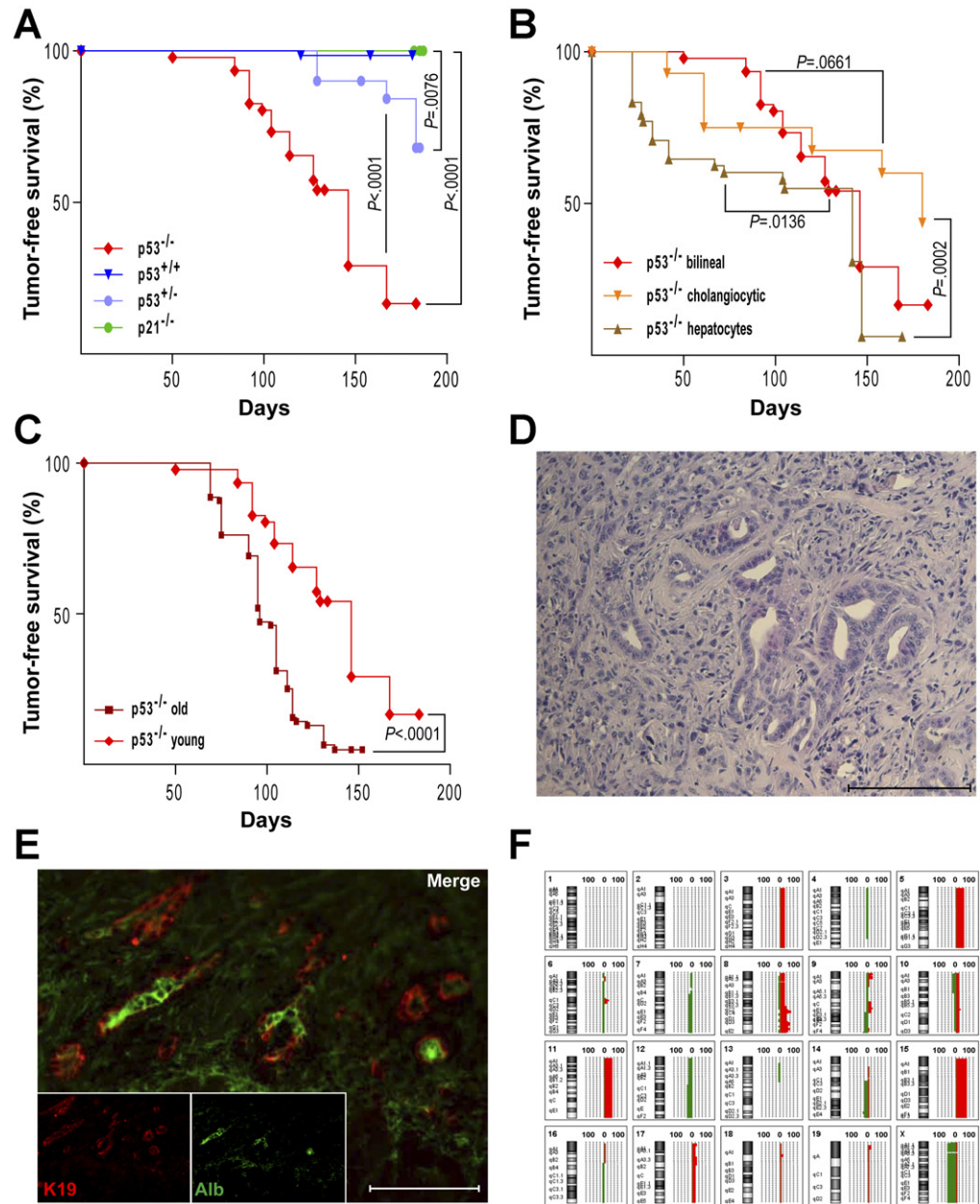
increased chromosomal instability of LPCs and hepatocytes.

p53 Deletion Induces Transformation of LPCs and Hepatocytes

Because liver tumors in p53^{-/-} livers showed a mixed differentiation, tumor-forming capacity of bipo-

tent LPCs and hepatocytes were analyzed. Immunocompromised mice were subcutaneously injected with primary cultures derived from bipotent or cholangiocytic progenitor cells or hepatocytes of 2- to 3-month-old mice. Primary cultures from all 3 cell types exhibited robust tumor-forming capacity when isolated from p53^{-/-} liver, whereas cultures from bipotent progenitor cells of wild-

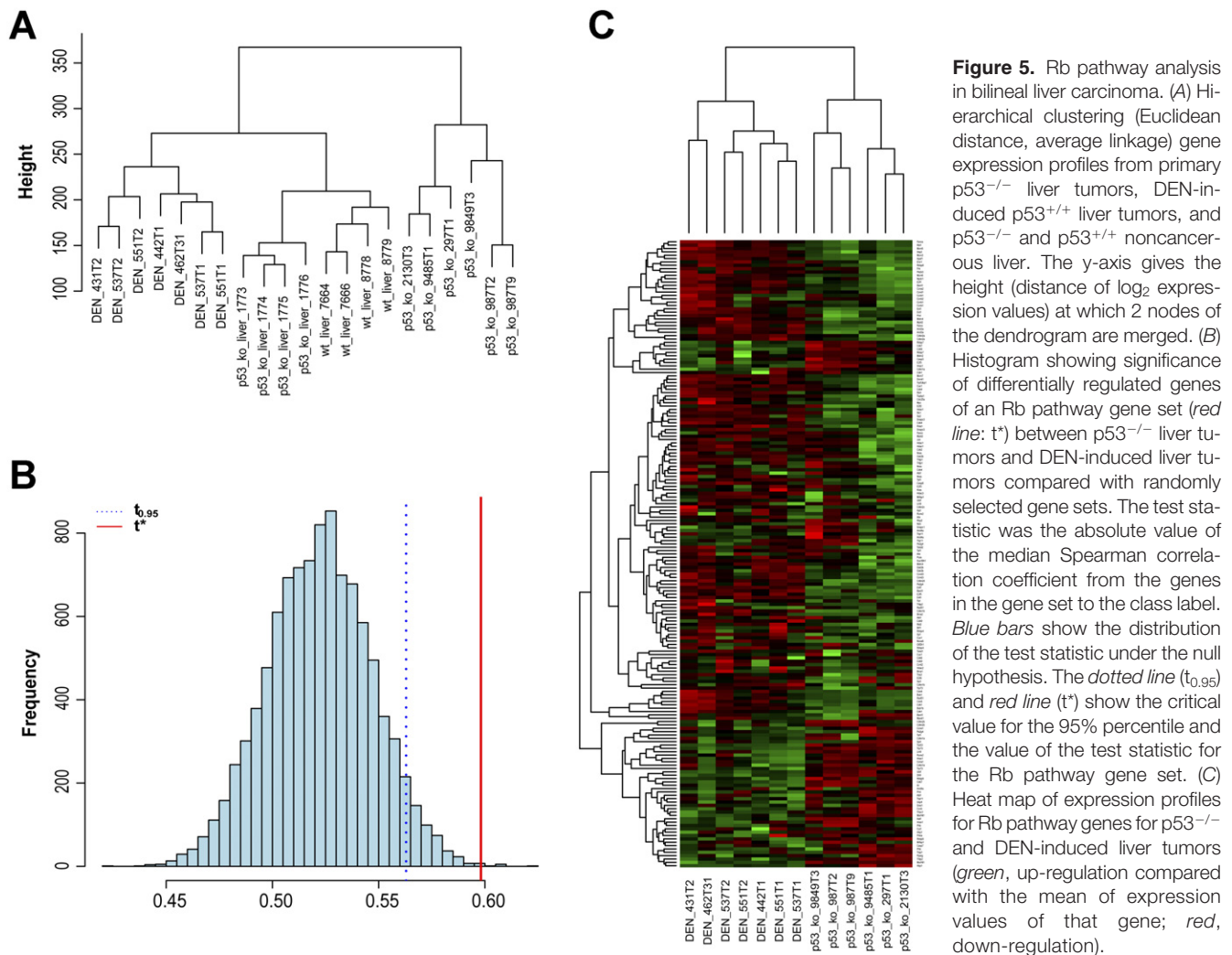
Figure 4. p53 deletion leads to transformation of liver cells. (A) Tumor-free survival curve of immunocompromised (NOD-scid IL2Rg^{null}) mice that underwent transplantation with LPC cultures with bilineal differentiation from 2- to 3-month-old p53^{-/-} (n = 28/46), p53^{+/+} (n = 1/64), p53^{+/-} (n = 11/40), or p21^{-/-} (n = 0/40) donors. (B) Tumor-free survival curve of recipient mice that underwent transplantation with LPC cultures with bilineal (n = 28/46) and cholangiocytic differentiation (n = 14/28), or hepatocyte cultures with bilineal differentiation (n = 32/48) from 2- to 3-month-old p53^{-/-} donors. (C) Tumor-free survival curve of recipient mice that underwent transplantation with LPC cultures with bilineal differentiation from 2- to 3-month-old (n = 28/46) and 8- to 10-month-old (n = 80/88) p53^{-/-} donors. (D) H&E staining of the tumors in recipient mice revealed a similar morphology compared with the primary liver tumors with bilineal differentiation in p53^{-/-} mice. (E) Immunofluorescence showing expression of hepatocytic (albumin) and cholangiocytic marker (K19) in a tumor. Scale bars = 100 μm. (F) Ideogram summarizes genomic imbalances (gains, red; losses, green) in tumors derived from p53^{-/-} LPCs with bilineal differentiation.



type, p53^{+/-}, or p21^{-/-} mice exhibited a much lower tumor-forming capacity (Figure 4A-C). As indicated previously, hepatocytes did not grow in culture from p53^{+/+} donors. Within the p53^{-/-} cell lines, cells derived from cholangiocytic progenitor cells exhibited a slightly reduced tumor-forming capacity compared with cells derived from bipotent progenitor cells (14/28; Figure 4B) and hepatocyte cultures exhibited slightly increased tumor-forming capacity (Figure 4B). Compared with these results on primary cell cultures, freshly isolated hepatocytes exhibited a strongly reduced tumor-forming capacity (1/40; data not shown). The number of freshly isolated progenitor cells was too low (1000–2000 cells per mouse) to determine the tumor-forming capacity of freshly isolated, noncultured cells. Although the culture conditions had little effect on chromosomal instability in these cells

(Figure 3B), it is possible that culture conditions impacted on the tumorigenic potential. Comparing the tumorigenic potential of primary cultures derived from bipotent LPCs of 2- to 3- or 8- to 10-month-old p53^{-/-} mice revealed a significant donor age-dependent increase in the tumorigenic potential, indicating that age-dependent in vivo processes contributed to transformation of these progenitor cells (Figure 4C).

The tumors in immunocompromised mice morphologically resembled primary tumors developing in livers of aging p53^{-/-} mice exhibiting a high stromal content and a mixed differentiation with hepatocytic (albumin) and cholangiocytic (K19) differentiation (Figure 4D and E). Moreover, aCGH analysis of the tumors showed chromosomal aberrations that partly overlapped with those in primary tumors and in progenitor cells from p53^{-/-} livers (Figure 4F and Supplementary Figure 7).



Together, these results indicated that liver tumors with bilineal differentiation in p53^{-/-} mice can originate from cholangiocytic or bipotent LPCs as well as from hepatocytes with a changed differentiation status after in vitro culture.

Liver Carcinogenesis in p53-Deficient Mice Associates With Complex Dysregulation of Rb Pathway Genes

Recent studies reported that p53 deletion cooperates with Rb dysfunction in the induction of liver tumor formation.⁴⁵ To analyze whether Rb checkpoint function was involved in the development of liver tumors in response to p53 deletion, we analyzed gene expression profiles from spontaneous bilineal liver tumors of p53^{-/-} mice compared with DEN-induced HCCs from p53^{+/+} mice (Figure 5). Hierarchical clustering analysis revealed that p53^{-/-} tumors clustered separately from DEN-induced tumors (Figure 5A). Pathway enrichment analysis of 122 genes involved in the Rb pathway (Supplementary Table 3) resulted in strong separation of p53^{-/-} liver tumors from DEN-induced liver tumors (Figure 5C). Of note, the Rb checkpoint genes were significantly more powerful in separating liver tumors from p53^{-/-} versus p53^{+/+} livers compared with random chosen gene data

sets (Figure 5B). To investigate an inhibitory or excitatory behavior of the Rb pathway, we performed a literature-based grouping of genes involved in the Rb pathway into indicators of Rb checkpoint activation ("Rb active"; n = 36 of 123) or into indicators of Rb checkpoint inactivation ("Rb inactive"; n = 56 of 123). No statistical difference in proportions of positive versus negative regulated genes of these 2 groups was detected in liver tumors of p53^{+/+} versus p53^{-/-} mice (Fisher exact test [2-sided]; P = .3687). These data indicated that differential regulation of Rb checkpoint genes was strongly associated with liver tumor formation in p53^{-/-} versus p53^{+/+} mice, but this difference in gene regulation was complex and not strictly indicative of Rb checkpoint activation or inactivation.

Discussion

The current study provides the first experimental evidence that p53 deletion as a single genetic lesion induces liver tumors with high penetrance. These data represent the first example for a solid organ where p53 deletion is sufficient to induce tumorigenesis while germline p53^{-/-} mice mainly develop lymphomas and sarcoma

mas.⁴⁶ The limited life span of germline p53-deficient mice did not allow studying tumor formation in a solid organ system. Other studies on organ-specific deletion in conditional knockout mice revealed that p53 deletion is not sufficient to induce tumors in brain and intestine.^{43,47} These results indicate that organ-specific differences with regard to the role of p53 in tumor development exist and that loss of p53 per se does not lead to tumor formation in all organs. The current finding that loss of p53 by itself can represent a tumor-initiating lesion in the liver is of particular interest because p53 mutations represent an early lesion in aflatoxin B-induced liver cancer.¹⁶⁻¹⁸ In contrast, p53 mutations represent a late event in other tumor types, such as intestinal carcinoma.⁴⁸ It is conceivable that organ-specific differences in the tumorigenic potential of p53 mutations select for a different order of genetic events and different tumor-initiating events.

This study shows that p53^{-/-} tumors exhibit a mixed differentiation with hepatocytic and cholangiocytic features. Interestingly, there is emerging evidence that loss of p53 function is associated with stem cell-specific gene expression signatures in human HCC.^{10,11} Together with our current mouse model, these findings support a novel concept indicating that loss of p53 function may predispose to the development of dedifferentiated liver tumors exhibiting bilineal differentiation and stem cell features. A possible explanation for these findings could be that p53 deletion leads to tumor formation originating from liver stem/progenitor cells. A variety of previous studies have shown that p53 deletion can increase stem cell self-renewal in various tissues.⁷⁻⁹ p53 deletion also increased the efficiency to induce pluripotent stem cells (iPS cells).²⁻⁶ In addition, p53-dependent effects on progenitor cell transformation were reported in mouse models combining p53 deletion with other oncogenic mutations,^{13,14} possibly involving an aberrant enhancement of stem cell self-renewal by increases in symmetric stem cell divisions.⁴⁹ The current study suggests that p53 deletion may lead to a prolonged maintenance of the colony-forming capacity of bipotent LPCs during aging.

An alternative explanation for the formation of liver tumors with bilineal differentiation in response to p53 deletion is that loss of p53 function leads to transformation and changes in differentiation status of differentiated liver cells. The study shows that p53 deletion impairs induction of hepatocyte quiescence in vivo. In primary ex vivo cultures, loss of p53 function was required to establish hepatocyte cultures, but these cells quickly developed bilineal differentiation potential. These findings indicate that changed differentiation status and transformation of hepatocytes could contribute to the formation of bilineal liver tumors in response to p53 deletion.

The mechanisms that induce transformation of liver cells in response to p53 deletion remain to be defined. The current study indicates that both LPCs and hepatocytes gain tumorigenic potential in response to p53 deletion. It is possible that (1) an increase in self-renewal of bipotent progenitor cells and (2) a change in differentiation status of

hepatocytes contribute to formation of liver cancer with bilineal differentiation in response to p53 deletion. The induction of chromosomal imbalances could play a causal role in cellular transformation in both processes. The current study shows that both hepatocytes and LPC fraction accumulate chromosomal imbalances in response to p53 deletion.

It remains to be delineated which downstream targets of p53 restrict self-renewal of LPCs or alterations in differentiation status of hepatocytes. The current data indicate that the deletion of p21 does not lead to the same increase in self-renewal of bipotent LPCs or the transformation of hepatocytes compared with the deletion of p53. It is possible that other downstream targets of p53 (eg, Puma, 14-3-3 sigma, sestrins) may play a decisive role and that these p53-dependent pathways are differentially regulated in different tissues.

It was reported that the deletion of the p53 checkpoint and Rb checkpoint genes often cosegregate in human HCC, but deletion of the Rb pathway occurs mainly in advanced HCCs.^{50,51} In addition, p53 deletion cooperated with Rb checkpoint deletion in the induction of HCC in mouse models.⁴⁵ Our gene expression analysis supports the view that p53 deletion by itself is sufficient to induce liver carcinogenesis. The tumors exhibit a significant dysregulation of Rb checkpoint genes compared with DEN-induced liver tumors in p53^{+/+} mice. However, these alterations in Rb checkpoint function in p53-deficient liver tumors were complex and not strictly indicative of either activation or inactivation of the Rb checkpoint.

Together, the current study provides the first experimental evidence that p53 deletion leads to formation of liver tumors with bilineal differentiation associated with increases in progenitor cell self-renewal, alterations in hepatocyte differentiation status, and the evolution of genomic imbalances. Tumor development involved complex dysregulation of Rb checkpoint genes and was at least partially independent of p21 checkpoint function.

Supplementary Material

Note: To access the supplementary material accompanying this article, visit the online version of *Gastroenterology* at www.gastrojournal.org, and at doi: 10.1053/j.gastro.2012.02.009.

References

1. Vogelstein B, Lane D, Levine AJ. Surfing the p53 network. *Nature* 2000;408:307-310.
2. Lin T, Chao C, Saito S, et al. p53 induces differentiation of mouse embryonic stem cells by suppressing Nanog expression. *Nat Cell Biol* 2005;7:165-171.
3. Kawamura T, Suzuki J, Wang YV, et al. Linking the p53 tumor suppressor pathway to somatic cell reprogramming. *Nature* 2009;460:1140-1144.
4. Li H, Collado M, Villasante A, et al. The Ink4/Arf locus is a barrier for iPS cell reprogramming. *Nature* 2009;460:1136-1139.
5. Marion RM, Strati K, Li H, et al. A p53-mediated DNA damage response limits reprogramming to ensure iPS cell genomic integrity. *Nature* 2009;460:1149-1153.

6. Hong H, Takahashi K, Ichisaka T, et al. Suppression of induced pluripotent stem cell generation by the p53-p21 pathway. *Nature* 2009;460:1132–1135.
7. Meletis K, Wirta V, Hede SM, et al. p53 suppresses the self-renewal of adult neural stem cells. *Development* 2006;133:363–369.
8. Chen J, Ellison FM, Keyvanfar K, et al. Enrichment of hematopoietic stem cells with SLAM and LSK markers for the detection of hematopoietic stem cell function in normal and Trp53 null mice. *Exp Hematol* 2008;36:1236–1243.
9. Pearson BJ, Sanchez Alvarado A. A planarian p53 homolog regulates proliferation and self-renewal in adult stem cell lineages. *Development* 2010;137:213–221.
10. Nakano A, Watanabe N, Nishizaki Y, et al. Immunohistochemical studies on the expression of P-glycoprotein and p53 in relation to histological differentiation and cell proliferation in hepatocellular carcinoma. *Hepatol Res* 2003;25:158–165.
11. Woo HG, Wang XW, Budhu A, et al. Association of TP53 mutations with stem cell-like gene expression and survival of patients with hepatocellular carcinoma. *Gastroenterology* 2011;140:1063–1070.
12. Moretti F, Farsetti A, Soddu S, et al. p53 re-expression inhibits proliferation and restores differentiation of human thyroid anaplastic carcinoma cells. *Oncogene* 1997;14:729–740.
13. Zhao Z, Zuber J, Diaz-Flores E, et al. p53 loss promotes acute myeloid leukemia by enabling aberrant self-renewal. *Genes Dev* 2010;24:1389–1402.
14. Zheng H, Ying H, Yan H, et al. p53 and Pten control neural and glioma stem/progenitor cell renewal and differentiation. *Nature* 2008;455:1129–1133.
15. Molchadsky A, Rivlin N, Brosh R, et al. p53 is balancing development, differentiation and de-differentiation to assure cancer prevention. *Carcinogenesis* 2010;31:1501–1508.
16. El-Serag HB, Rudolph KL. Hepatocellular carcinoma: epidemiology and molecular carcinogenesis. *Gastroenterology* 2007;132:2557–2576.
17. Bressac B, Kew M, Wands J, et al. Selective G to T mutations of p53 gene in hepatocellular carcinoma from southern Africa. *Nature* 1991;350:429–431.
18. Aguilar F, Harris CC, Sun T, et al. Geographic variation of p53 mutational profile in nonmalignant human liver. *Science* 1994;264:1317–1319.
19. Laurent-Puig P, Legoix P, Bluteau O, et al. Genetic alterations associated with hepatocellular carcinomas define distinct pathways of hepatocarcinogenesis. *Gastroenterology* 2001;120:1763–1773.
20. Roskams T. Liver stem cells and their implication in hepatocellular and cholangiocarcinoma. *Oncogene* 2006;25:3818–3822.
21. Tang Y, Kitisin K, Jogunoori W, et al. Progenitor/stem cells give rise to liver cancer due to aberrant TGF-beta and IL-6 signaling. *Proc Natl Acad Sci U S A* 2008;105:2445–2450.
22. Durnez A, Verslype C, Nevens F, et al. The clinicopathological and prognostic relevance of cytokeratin 7 and 19 expression in hepatocellular carcinoma. A possible progenitor cell origin. *Histopathology* 2006;49:138–151.
23. Marquardt JU, Thorgeirsson SS. Stem cells in hepatocarcinogenesis: evidence from genomic data. *Semin Liver Dis* 2010;30:26–34.
24. Woo HG, Lee JH, Yoon JH, et al. Identification of a cholangiocarcinoma-like gene expression trait in hepatocellular carcinoma. *Cancer Res* 2010;70:3034–3041.
25. Jonkers J, Meuwissen R, van der Gulden H, et al. Synergistic tumor suppressor activity of BRCA2 and p53 in a conditional mouse model for breast cancer. *Nat Genet* 2001;29:418–425.
26. Kellendonk C, Opherck C, Anlag K, et al. Hepatocyte-specific expression of Cre recombinase. *Genesis* 2000;26:151–153.
27. Deng C, Zhang P, Harper JW, et al. Mice lacking p21CIP1/WAF1 undergo normal development, but are defective in G1 checkpoint control. *Cell* 1995;82:675–684.
28. Kamiya A, Kakinuma S, Yamazaki Y, et al. Enrichment and clonal culture of progenitor cells during mouse postnatal liver development in mice. *Gastroenterology* 2009;137:1114–1126.
29. Geigl JB, Speicher MR. Single-cell isolation from cell suspensions and whole genome amplification from single cells to provide templates for CGH analysis. *Nat Protoc* 2007;2:3173–3184.
30. Geigl JB, Obenauf AC, Waldispuehl-Geigl J, et al. Identification of small gains and losses in single cells after whole genome amplification on tiling oligo arrays. *Nucleic Acids Res* 2009;37:e105.
31. Naugler WE, Sakurai T, Kim S, et al. Gender disparity in liver cancer due to sex differences in MyD88-dependent IL-6 production. *Science* 2007;317:121–124.
32. Farazi PA, Glickman J, Jiang S, et al. Differential impact of telomere dysfunction on initiation and progression of hepatocellular carcinoma. *Cancer Res* 2003;63:5021–5027.
33. Evarts RP, Nagy P, Marsden E, et al. A precursor-product relationship exists between oval cells and hepatocytes in rat liver. *Carcinogenesis* 1987;8:1737–1740.
34. Petersen BE, Grossbard B, Hatch H, et al. Mouse A6-positive hepatic oval cells also express several hematopoietic stem cell markers. *Hepatology* 2003;37:632–640.
35. Singh SK, Clarke ID, Terasaki M, et al. Identification of a cancer stem cell in human brain tumors. *Cancer Res* 2003;63:5821–5828.
36. Shackleton M, Quintana E, Fearon ER, et al. Heterogeneity in cancer: cancer stem cells versus clonal evolution. *Cell* 2009;138:822–829.
37. Choudhury AR, Ju Z, Djojotubroto MW, et al. Cdkn1a deletion improves stem cell function and lifespan of mice with dysfunctional telomeres without accelerating cancer formation. *Nat Genet* 2007;39:99–105.
38. Cheng T, Rodrigues N, Shen H, et al. Hematopoietic stem cell quiescence maintained by p21cip1/waf1. *Science* 2000;287:1804–1808.
39. Donehower LA, Godley LA, Aldaz CM, et al. Deficiency of p53 accelerates mammary tumorigenesis in Wnt-1 transgenic mice and promotes chromosomal instability. *Genes Dev* 1995;9:882–895.
40. Liu G, Parant JM, Lang G, et al. Chromosome stability, in the absence of apoptosis, is critical for suppression of tumorigenesis in Trp53 mutant mice. *Nat Genet* 2004;36:63–68.
41. Chin L, Artandi SE, Shen Q, et al. p53 deficiency rescues the adverse effects of telomere loss and cooperates with telomere dysfunction to accelerate carcinogenesis. *Cell* 1999;97:527–538.
42. Artandi SE, Chang S, Lee SL, et al. Telomere dysfunction promotes non-reciprocal translocations and epithelial cancers in mice. *Nature* 2000;406:641–645.
43. Begus-Nahrmann Y, Lechel A, Obenauf AC, et al. p53 deletion impairs clearance of chromosomal-unstable stem cells in aging telomere-dysfunctional mice. *Nat Genet* 2009;41:1138–1143.
44. Sperka T, Song Z, Morita Y, et al. Puma and p21 represent cooperating checkpoints limiting self-renewal and chromosomal instability of somatic stem cells in response to telomere dysfunction. *Nat Cell Biol* 2011;14:73–79.
45. McClendon AK, Dean JL, Ertel A, et al. RB and p53 cooperate to prevent liver tumorigenesis in response to tissue damage. *Gastroenterology* 2011;141:1439–1450.
46. Jacks T, Remington L, Williams BO, et al. Tumor spectrum analysis in p53-mutant mice. *Curr Biol* 1994;4:1–7.
47. Marino S, Vooijs M, van Der Gulden H, et al. Induction of medulloblastomas in p53-null mutant mice by somatic inactivation of Rb in the external granular layer cells of the cerebellum. *Genes Dev* 2000;14:994–1004.

48. Vogelstein B, Fearon ER, Hamilton SR, et al. Genetic alterations during colorectal-tumor development. *N Engl J Med* 1988;319:525–532.
49. Cicalese A, Bonizzi G, Pasi CE, et al. The tumor suppressor p53 regulates polarity of self-renewing divisions in mammary stem cells. *Cell* 2009;138:1083–1095.
50. Staib F, Hussain SP, Hofseth LJ, et al. TP53 and liver carcinogenesis. *Hum Mutat* 2003;21:201–216.
51. Peng CY, Chen TC, Hung SP, et al. Genetic alterations of INK4alpha/ARF locus and p53 in human hepatocellular carcinoma. *Anticancer Res* 2002;22:1265–1271.

Received June 16, 2011. Accepted February 7, 2012.

Reprint requests

Address requests for reprints to: Prof. Dr. K. Lenhard Rudolph, Department of Molecular Medicine and Max Planck Research Group on Stem Cell Aging, University of Ulm, Albert-Einstein-Allee 11, 89081 Ulm, Germany. e-mail: lenhard.rudolph@uni-ulm.de.

Acknowledgments

S.-F.K. and A.L. contributed equally to this work.

The authors thank A. Berns (The Netherlands Cancer Institute, Amsterdam, The Netherlands) for providing conditional p53 knockout mice, G. Schütz (German Cancer Research Center, Heidelberg, Germany) for providing AlfpCre-transgenic mice, and V. Factor for providing the A6 antibody.

Conflicts of interest

The authors disclose no conflicts.

Funding

Supported by the Deutsche Forschungsgemeinschaft (KFO 167, RU745/10-1), the Deutsche Krebshilfe e.V. (consortium grant on tumor stem cells), and the European Union (GENINCA, Telomarker). S.-F.K. is supported by the Excellence Initiative of the German Federal and State Governments/DFG (International PhD Program in Molecular Medicine, University of Ulm), A.C.O. and E.M.H. by the Medical University of Graz (PhD Program “Molecular Medicine”), and D.H. by the Else Kröner-Fresenius-Stiftung (EKFS Memorial Scholarship). K.L.R. and M.R.S. are both supported by the European Union (GENINCA, contract number 202230).

Supplementary Materials and Methods

Histologic Analysis

Histologic analysis (immunohistochemistry, immunofluorescence) was performed on 5- μ m-thick paraffin sections of the tumors. Sections were deparaffinized, rehydrated, and permeabilized in 1 mmol/L sodium citrate. For immunofluorescence staining of cells grown on culture dishes, the cells were fixed with paraformaldehyde and permeabilized with 0.1% Triton X-100/0.1% sodium citrate. Samples were stained with primary antibodies at 4°C overnight or at room temperature for 2 hours: albumin (1:100; Bethyl Diagnostics, Montgomery, TX), CK19 (1:50; Santa Cruz Biotechnology, Santa Cruz, CA), A6 (1:10),¹ and CD133 (1:200; Abcam, Cambridge, England). The secondary antibodies were applied at room temperature for 1 hour.

DEN Treatment for the Induction of Liver Tumors

DEN (10 μ g/g body wt) was injected intraperitoneally at day 15 into p53^{+/+} (C57BL6J background) mice. The mice were killed at an age of 13–15 months.

UV Laser Microdissection and Quantitative Polymerase Chain Reaction for Analysis of p53 Gene Status

For analysis of p53 gene status, tumor and stroma cells were isolated from the same tumor via contact-free UV laser microdissection. Tissue was cryosectioned using a Leica CM 3050 S cryotome (Leica Microsystems, Wetzlar, Germany). Twelve-micrometer sections were mounted on UV-C sterilized PEN membrane slides (Leica Microsystems, Wetzlar, Germany) and H&E stained (1 minute of 70% EtOH, 30 seconds of H₂O, 1 minute of Mayer's hematoxylin, rinse in H₂O, 30 seconds of 70% EtOH, 30 seconds of 95% EtOH, 3 minutes of eosin, and 30 seconds of 95% EtOH). UV laser microdissection was performed essentially as described using a Leica LMD 6000 system (Leica Microsystems).² Each microdissected tissue piece consisted of approximately 10–15 cells. For each sample, a pool of 30 tissue areas was microdissected, 9 μ L H₂O was added, and the DNA was immediately amplified using the GenomePlex single cell whole genome amplification kit WGA4 (Sigma-Aldrich, St Louis, MO). The amplified DNA was used to analyze the percentage of deleted and wild-type/floxed p53. Specific primers were used detecting only deleted p53 (forward, 5'-CGTCCTTTTCGCAATCCTTTATTC-3'; reverse, 5'-CACCATCACCATGAGACAGG-3'; size of product, 199 base pairs) or only wild-type/floxed p53 (forward, 5'-AACGACCTGGAAGATAGAGC-3'; reverse, 5'-TTCACCCTGTCAAGGAAGACTC-3'; size of product, 162 base pairs). Quantitative real-time polymerase chain reaction (PCR) was performed with an ABI 7300 Real-Time PCR System (Applied Biosystems, Carlsbad, CA).

Isolation of Side Population Cells

Cells were stained with 5 μ g/mL Hoechst 33342 dye (Sigma-Aldrich) in Dulbecco's modified Eagle medium for 90 minutes at 37°C. For control, the dye efflux was blocked with 50 μ mol/L verapamil (Sigma-Aldrich). After excluding debris, doublets, and dead cells, side population cells (Hoechst negative) and non-side population cells (Hoechst positive) were sorted on a BD FACS Aria II flow cytometer (BD Biosciences, San Jose, CA).

Isolation of Adult Mouse LPCs

Liver cells were isolated from postnatal mouse livers by 2-step collagenase perfusion. LPCs were isolated as described previously.³ Nonparenchymal cells (including LPCs) were separated from mature hepatocytes (parenchymal cells) by low-speed centrifugation (50g for 1 minute). After removing dead cells by centrifugation in 25% Percoll solution (GE Healthcare, Amersham, England) and 2 washing steps with phosphate-buffered saline (containing 2% fetal bovine serum), the nonparenchymal cells were stained for 1 hour with the following anti-mouse antibodies: CD13-PE, CD49f-FITC, TER119-PE-Cy7 (BD Biosciences, San Jose, CA), CD133-APC, CD45-PE-Cy7, Sca1-PE-Cy7, and cKit-PE-Cy7 (eBiosciences, San Diego, CA). After excluding debris, doublets, and dead cells, adult LPCs (CD45⁻, TER119⁻, cKit⁻, Sca1⁻, CD13⁺, CD133⁺, CD49f⁺) were analyzed and sorted on a BD FACS Aria II flow cytometer.

In Vitro Colony-Forming Assay

Nonparenchymal LPCs were cultured as described previously.³ The standard medium consisted of 50% conditioned medium derived from E14.5 fetal liver cells and 50% Dulbecco's modified Eagle medium/F12 with 10% fetal bovine serum, 1 \times Insulin-Transferrin-Selenium X, 10 mmol/L nicotinamide, 10⁻⁷ mol/L dexamethasone, 2.5 mmol/L HEPES, 1 \times penicillin/streptomycin/L-glutamine, and 1 \times nonessential amino acid solution. Cells were incubated in this standard medium in the presence of 40 ng/mL hepatocyte growth factor (PeproTech, Rocky Hill, NJ), 20 ng/mL epidermal growth factor (PeproTech), and 20 μ mol/L Y-27632 (Rho-associated kinase inhibitor; Ascent Scientific, Bristol, England).

Cultivation of Hepatocytes

Hepatocytes were cultivated on collagen type I-coated plates in standard Dulbecco's modified Eagle medium containing 10% fetal bovine serum, 1 \times Insulin-Transferrin-Selenium X, 10⁻⁷ mol/L dexamethasone, 1 \times penicillin/streptomycin/L-glutamine, and 1 \times nonessential amino acid solution.

Genome-Wide Amplification

Genome-wide amplification of DNA was performed as described previously.⁴ The GenomePlex single cell whole genome amplification kit WGA4 (Sigma-Al-

drich) was used according to the manufacturer's instructions with the following modifications. After cell lysis and fragmentation of the genomic DNA, an amplification of the libraries was performed by adding 6 μ L of 10 \times amplification master mix, 36 μ L of nuclease-free water, and 4 μ L WGA DNA polymerase to 14 μ L library mix. PCR conditions for amplification were denaturation at 95°C for 3 minutes followed by 25 cycles, with each cycle consisting of a denaturation step at 94°C for 30 seconds and an annealing and extension step at 65°C for 5 minutes. DNA was purified using the Wizard SV Gel and PCR Clean-Up System (Promega, Madison, WI). The quality of the amplification was evaluated using a multiplex PCR approach as previously described.⁵

Bromodeoxyuridine Treatment of Mice

Mice were continuously labeled with bromodeoxyuridine (BrdU; Sigma-Aldrich) in the drinking water (0.8 mg/mL) for 7 to 28 days. Drinking water was replaced every 24 hours.

BrdU Staining of Hepatocytes

Freshly purified hepatocytes from BrdU-labeled mice were fixed with 70% ethanol and stained for BrdU incorporation with an anti-BrdU fluorescein isothiocyanate-labeled antibody (BD Biosciences) according to the manufacturer's protocol. The cells were analyzed on a BD FACS LSRII flow cytometer.

BrdU Staining of LPCs

Freshly isolated adult LPCs from BrdU-labeled mice were sorted on a poly-L-lysine-coated glass slide. The cells were fixed with 70% ethanol. DNA was denatured with 4N HCl/0.5% Tween 20 for 15 minutes. Afterward, the cells were stained with an anti-BrdU Alexa Fluor 488-labeled antibody (Invitrogen, Carlsbad, CA). The cells were analyzed on a Leica fluorescence microscope.

Terminal Deoxynucleotidyl Transferase-Mediated Deoxyuridine Triphosphate Nick-End Labeling (TUNEL) Staining of Cultured Hepatocytes

Cells were stained using the In Situ Cell Death Detection Kit, Fluorescein (Roche Applied Science, Indianapolis, IN) according to the manufacturer's protocol.

RNA Isolation

Total RNA was isolated from shock frozen tissue by using RNeasy Lys R (Qiagen, Valencia, CA) according to the manufacturer's protocol. For microarray analysis, total RNA was isolated using the RNeasy Mini Kit (Qiagen, Valencia, CA) according to the manufacturer's instructions. The quality of the RNA was analyzed with the 2100 Bioanalyzer (Agilent Technologies, Santa Clara, CA). Samples with a RIN factor >5.9 were used for further analysis.

Quantitative Real-Time PCR

Quantitative real-time PCR was performed with an ABI 7300 Real-Time PCR System (Applied Biosystems) in triplicate from at least 4 biological samples. The Superscript III Kit (Invitrogen) was used for complementary DNA synthesis. TaqMan assays for CD133 and CD90 (Applied Biosystems) were performed in a volume of 25 μ L.

Rb Pathway Gene List

A set of genes related to the Rb pathway (upstream genes, interaction partners, downstream targets) was established for comparison of gene expression data from p53^{-/-} liver tumors and p53^{+/+} DEN-induced liver tumors. Genes were selected from published data using the PubMed database. A detailed list of selected genes is specified in Supplementary Table 3. The corresponding references are listed in the Supplementary References for the Rb pathway gene list. To investigate an inhibitory or excitatory behavior of the Rb pathway, we performed a literature-based grouping of the Rb-related genes into indicators for an active Rb pathway ("Rb-active"; n = 36 of 123) or into indicators for an inactive Rb pathway ("Rb-inactive"; n = 56 of 123). Due to conflicting literature reports, 31 genes could not be assigned to either group. Detailed lists for these 2 groups are available as Supplementary Tables 4 and 5.

Analysis of Gene Expression Data

Expression data were extracted using the Feature Extraction software (Agilent Technologies). Preprocessing of expression data was performed according to Agilent's standard workflow. Using 5 quality flags (gIsPosAndSignif, gIsFeatNonUnifOL, gIsWellAboveBG, gIsSaturated, and gIsFeatPopnOL) from the Feature Extraction software output, probes were labeled as detected, not detected, or compromised. Gene expression levels were background corrected, and signals for duplicated probes were summarized by geometric mean of noncompromised probes. After log₂ transformation, a percentile shift normalization at the 75% level and a baseline shift to the median baseline of all probes was performed. All computations were performed using the R statistical software framework (<http://www.R-project.org>).

Hierarchical clustering with Euclidean distance and average linkage was performed using all available probe sets and is shown as a dendrogram. Expression pattern of Rb pathway genes (Supplementary Table 3) is shown as a heat map for DEN and p53 knockout samples. Gene set enrichment analysis was performed as described as follows.⁶ The amount of differential expression of the individual genes (gene level statistics) was measured by Spearman correlation coefficient. The bias from using multiple probe sets targeting the same genes was adjusted by summarizing the different probe sets. The mean absolute value of single gene statistics was used as the gene set

statistic and was compared with the null hypothesis of no association of genes to the phenotype. Computer-intensive Monte Carlo simulation (gene sampling) was performed to assess the significance of the observed gene set statistic. Results from simulations are shown as a histogram, including the result for the Rb pathway gene set.

Supplementary Results

aCGH Analysis of Primary Liver Tumors in Conditional p53^{-/-} Mice and in DEN-Treated Mice

p53-deleted liver tumors showed a distinct pattern of chromosomal aberrations; the chromosomes 9, 12, and 15 were mainly affected, whereas DEN-induced liver tumors showed only a few aberrations with a random pattern, and a dominance was only recognized in a partial gain of chromosome 12.

aCGH Analysis of LPCs and Hepatocytes

We analyzed chromosomal aberrations in single cell-sorted LPCs as well as in colonies derived from single cell-sorted LPCs from p53^{-/-}, p53^{+/-}, p53^{+/+}, and p21^{-/-} mice. Aberrations were mainly found in the p53^{-/-} cells. The gains of genomic material from p53^{-/-} single cell-sorted LPCs were present in the X chromosome (14%), chromosome 7 (7.1%), and chromosomes 3, 5, 10, 11, and 17 (3.6%), and losses were present in the chromosomes 5, 6, and 12 (7.1%) and chromosomes 1, 2, 9, 10, 13, and 16 (3.6%). In p21^{-/-} single cell-sorted LPCs, only gains in chromosomes 6 and X (6.7%) were found. No aberrations were detected in single cell-sorted p53^{+/-} and p53^{+/+} LPCs.

The number of detected aberrations increased in the colonies that were grown from single cell-sorted LPCs. In p53^{-/-} colonies, gains were found in chromosome 15 (15%), chromosomes 1, 3, and 19 (10%), and chromosomes 5, 10, 12, and 17 (5%). Losses were present in chromosome 12 (20%), chromosome 11 (10%), and chromosomes 3, 5, 7, 8, 9, 10, 14, 17, and 18 (5%). In p21^{-/-} colonies, one gain of chromosome 6 (8.3%) and one loss of chromosome 11 (8.3%) were recognized. In the p53^{+/-} and p53^{+/+} colonies, only one sample showed a loss of chromosome 11 (6.3%). The aberrations in chromosomes 12 and 15 were the most prominent ones in the p53^{-/-} colonies. These aberrations were also the most detected ones in the p53^{-/-} primary liver tumors besides chromosome 9.

In single analyzed hepatocytes of p53^{-/-} mice, we detected only losses of chromosomes 4 and 11 (8%) and chromosomes 7, 8, 10, 15, and 17 (4%).

Supplementary References

1. Engelhardt NV, Factor VM, Yasova AK, et al. Common antigens of mouse oval and biliary epithelial cells. Expression on newly formed hepatocytes. *Differentiation* 1990;45:29–37.
2. Grundemann J, Schlaudraff F, Liss B. UV-laser microdissection and mRNA expression analysis of individual neurons from postmortem Parkinson's disease brains. *Methods Mol Biol* 2011;755:363–374.
3. Kamiya A, Kakinuma S, Yamazaki Y, et al. Enrichment and clonal culture of progenitor cells during mouse postnatal liver development in mice. *Gastroenterology* 2009;137:1114–1126.
4. Geigl JB, Speicher MR. Single-cell isolation from cell suspensions and whole genome amplification from single cells to provide templates for CGH analysis. *Nat Protoc* 2007;2:3173–3184.
5. Geigl JB, Obenaus AC, Waldispuehl-Geigl J, et al. Identification of small gains and losses in single cells after whole genome amplification on tiling oligo arrays. *Nucleic Acids Res* 2009;37:e105.
6. Ackermann M, Strimmer K. A general modular framework for gene set enrichment analysis. *BMC Bioinformatics* 2009;10:47.